MODELING THE SHAPE OF COHERENT THz PULSES EMITTED BY SHORT BUNCHES IN AN ELECTRON STORAGE RING*

A.-S. Müller, S. Casalbuoni, M. Fitterer, E. Huttel, Y.-L. Mathis, Karlsruhe Research Center, Germany
M. Schmelling, Max Planck Institute f. Nuclear Physics, Heidelberg, Germany

Abstract

A sufficiently short electron bunch will emit coherent synchrotron radiation of wavelengths equal to or larger than the bunch length. The shape of the emitted THz pulse depends amongst other things on the original shape and length of the bunch's charge distribution. A Michelson interferogram of the THz signal therefore contains information on the generating bunch. However, systematic effects make a bunch length measurement based on that technique non-trivial. In order to understand the variables involved, an analytical model of the pulse generation is needed. In this paper, a derivation of the THz pulse shape form first principles with special emphasis in the time domain is presented. The impact of the charge distribution of the Michelson interferogram is discussed.

INTRODUCTION

In classical electrodynamics the radiation field of an electron bunch at a storage ring can be calculated rigorously from the retarded potentials of the charge distribution. Here a simplified approach is presented, describing the radiation emitted in the direction of motion of the electrons by a solution of the 1-dimensional scalar wave equation $(c^2\partial_x^2 - \partial_t^2)E(x,t) = 0$. The bunch is modeled as a continuous charge distribution. Only the coherent part of the radiation field is considered in this approach, in contrast to the alternative (e.g. [1]), where also the incoherent emission is taken into account. Otherwise the two methods are equivalent. In a first step the expected time structure of the emitted THz pulse is calculated as a function of the longitudinal shape of the bunch. From the pulse an expression of the Michelson interferogram is derived. Finally, results for the special case of a gaussian charge distribution are compared with actual measurements performed at the ANKA storage ring and used to extract the RMS-bunchlength and the cutoff frequency of the detector/beam line system from the data.

MATHEMATICAL FRAMEWORK

With $s(\omega)$ the amplitude spectrum emitted by a point charge and $\rho(x)$ the charge density of a single bunch, the time structure for the field of a THz pulse can be written as a superposition of plane waves over the charge distribution of the bunch. The general result for a real-valued field

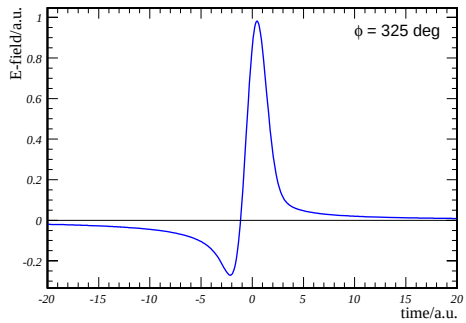

Figure 1: Example for the time structure of a THz pulse.

becomes

$$E(t) \sim \cos\phi \cdot \mathrm{Re}A(t) + \sin\phi \cdot \mathrm{Im}A(t) \qquad (1)$$

with

$$A(t) = \int_0^\infty d\omega \int_{-\infty}^\infty dx\; s(\omega)\,\rho(x)\,e^{-i\omega(t-x/c)}\;. \qquad (2)$$

and a phase factor ϕ which is not fixed a priori. For a given experimental setup ϕ is determined by the local acceleration of the emitting electrons, i.e. is a function of the storage ring optics. In case of synchrotron radiation and for low frequencies the point charge spectrum can be described as $s(\omega) \propto \omega^{1/6}$, corresponding to the well known power spectrum $s^2(\omega) \propto \omega^{1/3}$. The coherence condition is encoded through the phase factor $e^{-i\omega(t-x/c)}$ which suppresses all wavelengths larger than the bunch length when integrating over x. An example for the time structure of a pulse from a gaussian bunch is shown in Fig. 1. The time integral over the electric field vanishes as expected. For a phase $\phi = 0$ the pulse would be symmetric around $t = 0$.

Given the pulse $E(t)$ in the time domain, the interferogram obtained from a Michelson interferometer is given by the autocorrelation function

$$I(\delta) \sim \int dt |E(t) + E(t+\delta)|^2 \qquad (3)$$

with δ the difference in propagation times between the two arms of the spectrometer. For practical applications it is useful to work with normalized interferograms, which are scaled and shifted such that $I_N(\delta = 0) = 1$ and $I_N(\delta \to \pm\infty) = 0$. After some algebra the above expressions yield

$$I_N(\delta) = \frac{J(\delta)}{J(0)} \qquad (4)$$

with

$$J(\delta) = \int_0^\infty d\omega\; s^2(\omega)|\hat{\rho}(\omega/c)|^2\cos(\omega\delta)\;. \qquad (5)$$

* This work has partly been supported by the Initiative and Networking Fund of the Helmholtz Association under contract number VH-NG-320.

The function $\hat{\rho}(\omega/c)$ is the form factor of the bunch, i.e. the Fourier transform of the charge density. The result is independent of the unknown phase ϕ, and also allows an easy implementation of an experimental filter function $G_f(\omega)$ that multiplies the power spectrum $s^2(\omega)$.

GAUSSIAN BUNCH PROFILES

Gaussian charge densities are an important case in practical application. For Gaussian bunches, an analytical solution exists for the normalized interferogram, given by Kummer's confluent hypergeometric function

$$I_N(\delta) = {}_1F_1\left(\frac{2}{3}, \frac{1}{2}, -\frac{\delta^2 c^2}{4\sigma^2}\right) , \qquad (6)$$

where σ is the RMS-width of the charge distribution. This function is symmetric around $\delta = 0$, featuring a single central peak with an undershoot on both sides before relaxing to zero at $\delta \to \pm\infty$. Experimentally measured interferograms, on the other hand, usually show several oscillations before settling down. To account for this, bandwidth limitations have to be in incorporated into the model. In this paper a filter function having two free parameters is chosen,

$$G_f(\omega) = \left(1 - e^{-(\omega/\omega_k)^2}\right)^n , \qquad (7)$$

with a cutoff frequency ω_k and a power n, in the following referred to as "order", which allows to adjust the steepness of the filter step. Equation (7) is zero for $\omega = 0$ and approaches unity for large frequencies. It acts as a high pass filter and thus allows to model the suppression of low frequencies caused e.g. by aperture limits of the experimental setup. A similar ansatz is possible for a low-pass filter. However, since the coherence condition for the emission of the THz pulse effectively acts as a low-pass filter, an additional filter function has only very little impact on the shape of the interferogram and will not be discussed in the following. For a comparison with experimental data it is convenient to express the cutoff frequency as a function of n and a cutoff wave-number k, where G_f reaches 50% transmission.

$$w_k = \frac{2\pi k c}{\sqrt{-\ln(1 - 2^{-1/n})}} \qquad (8)$$

The filter function Eq.(7) allows to describe the interferogram in closed form. Introducing the dimensionless variables $x = \delta c/\sigma$ and $\mu = c/(\sigma\omega_k)$ the result reads

$$J(\delta) = \sum_{m=0}^{n} (-1)^m \binom{n}{m} \left(1 + m\mu^2\right)^{-2/3} f_m(x, \mu) \qquad (9)$$

with

$$f_m(x, \mu) = {}_1F_1\left(\frac{2}{3}, \frac{1}{2}, -\frac{x^2/4}{1 + m\mu^2}\right) . \qquad (10)$$

COMPARISON WITH EXPERIMENTAL DATA

The framework developed above shall be compared to a measurement of coherent synchrotron radiation from short bunch operation of the ANKA storage ring at a beam energy of 1.6 GeV [2]. In Fig. 2 the measured interferogram after correction for thermal radiation and incoherent synchrotron radiation is compared to the model without low-frequency cutoff. The width of the blue band shows the systematic errors of the measurement, which for this study were symmetrized around $\delta = 0$. Adjusting the bunch length parameter to $\sigma = 0.070$ mm, a reasonable description of the central peak is obtained. The oscillations in the data, however, are not reproduced.

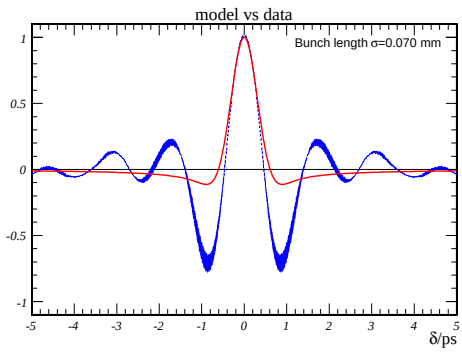

Figure 2: Measured interferogram (blue) compared to a model (red) without low-frequency cutoff.

The effect of the filter function on the interferogram is illustrated by Figs. 3 and 4. The first one shows how the oscillations in the interferogram get more and more pronounced with increasing the cutoff k. The first undershoot becomes deeper and the width of the central peak shrinks thus influencing a naive determination of the bunch length form the central peak's FWHM. As shown in Fig. 3, the order of the filter has relatively little impact on the shape of the interferogram, i.e. the dominant parameters are the RMS-bunchlength and the low frequency cutoff.

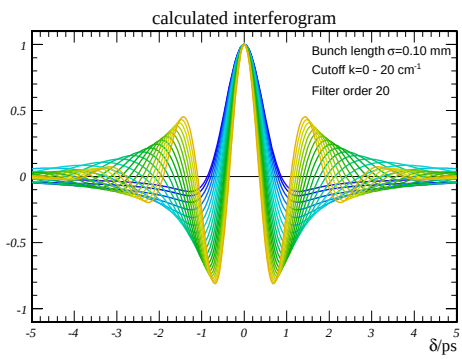

Figure 3: Evolution of the interferogram as a function of the low-frequency cutoff (blue: low orders, yellow: high orders).

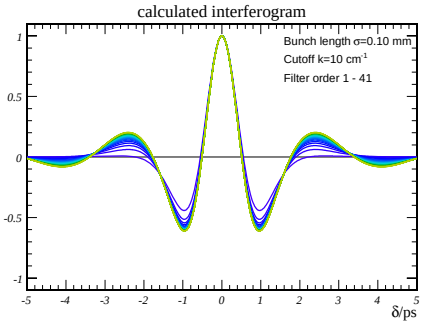

Figure 4: Evolution of the interferogram as a function of the order of the filter function.

For comparison and as a reference, the THz spectrum recorded for the data shown in Fig.2 has been used to extract the bunch length (details of the method can be found in [3]). In this approach, normalizing the coherent signal to the incoherent one, the filter function cancels out and the effective bunch length can be extracted from the spectral width. As shown in Fig. 5, the high frequency part of the data is reasonably well described by a simple Gaussian spectrum. The spectral width of $9\,\mathrm{cm}^{-1}$ translates to an effective RMS-bunchlength of $\sigma = 0.125\,\mathrm{mm}$.

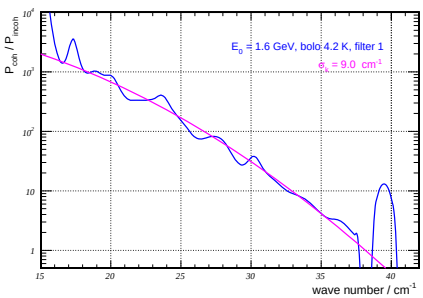

Figure 5: Extraction of the bunch length from the spectral with of the CSR signal.

The filter characteristics of the setup used for that measurement was determined by recording the spectrum of a Hg-Lamp using the identical detector setup. After dividing by the black body spectrum and normalizing the maximum to unity, the resulting filter function is shown in Fig. 6. Also shown is a parameterization according to the functional form Eq.(7), adjusted such that it roughly matches the 50% transmission point of the actual filter and the saturation towards large wave numbers. The obtained parameter settings are $k = 21\,\mathrm{cm}^{-1}$ and $n = 3$.

Using this filter function and an RMS-bunchlength of $\sigma = 0.125\,\mathrm{mm}$, the central peak, the first undershoot and the maximum of the following overshoot of the interferogram are already well reproduced by the analytical model derived above (see Fig.7). A full understanding of the entire interferogram will require to incorporate the details of the setup's filter function and possibly a non-gaussian charge distribution in the bunch.

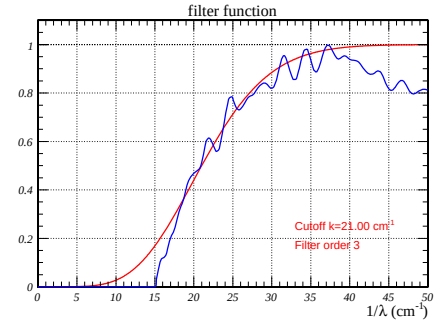

Figure 6: Filter function used in the model (red) in comparison to the filter characteristics inferred from the spectrum of the Hg-lamp.

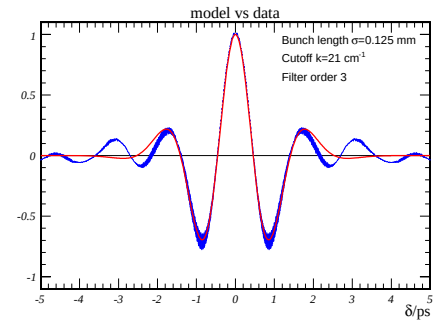

Figure 7: Data versus model with frequency cutoff.

SUMMARY AND OUTLOOK

An analytical expression for the Michelson interferogram from coherent synchrotron radiation has been derived from first principles. The model allows to include low frequency cutoffs. Comparison with experimental data shows that the basic features of the data are described by the model. The model allows to extract the bunch length together with the cutoff frequency of the measuring setup. The results are in good agreement with independent determinations of those parameters. Further improvements are expected from a numerical treatment, using the actual filter function and taking into account a non-gaussian charge distribution in the bunch.

ACKNOWLEDGMENTS

Useful discussions with B. Gasharova and D. Moss are gratefully acknowledged. We appreciated the kind help of I. Birkel, M. Süpfle and P. Wesolowski in measuring the interferograms.

REFERENCES

[1] H. Wiedemann, Particle Accelerator Physics, volume I.

[2] A.-S. Müller *et al.*, Beam Studies with Coherent Synchrotron Radiation from Short Bunches in the ANKA Storage Ring, Proceedings of the 10th European Particle Accelerator Conference, 2006.

[3] J. Feikes *et al.*, The BESSY Low Alpha Optics and the Generation of Coherent Synchrotron Radiation, ICFA Beam Dynamics Newsletter No. 35, December 2004, 2004.